Supplemental Information for

Complement and inflammasome overactivation mediates paroxysmal nocturnal hemoglobinuria with autoinflammation

Britta Höchsmann[+], Yoshiko Murakami[+], Makiko Osato[+], Alexej Knaus, Michi Kawamoto, Norimitsu Inoue, Tetsuya Hirata, Shogo Murata, Markus Anliker, Thomas Eggerman, Marten Jäger, Ricarda Floettmann, Alexander Höllein, Sho Murase, Yasutaka Ueda, Jun-ichi Nishimura, Yuzuru Kanakura, Nobuo Kohara, Hubert Schrezenmeier*, Peter M. Krawitz*, and Taroh Kinoshita*

[+]Equally contributed authors; *equally contributed corresponding authors.

This PDF file includes:

> Supplemental text
> Figures S1 to S8
> Tables S1 to S2
> References for Supplemental Information reference citations

Supplemental Methods
Blood samples and flow cytometry
Total peripheral blood cells were collected by centrifugation and a small sample was saved for staining erythrocytes. Total blood cells were subjected to hypotonic lysis in 40 volumes of ACK buffer to lyse erythrocytes and the remaining total leukocytes were washed with FACS buffer by centrifugation. Peripheral blood leukocytes were stained for GPI-anchored proteins (GPI-APs). Erythrocytes and reticulocytes were stained by anti-CD58 (clone AICD58, Beckman Coulter) or -CD59 (clone p282/H19, BD). Lymphocytes, monocytes and granulocytes were differentiated based on forward and side scatters (Figure S1**B**). In the lymphocytes gate, B- and T-lymphocytes were further gated by CD19- or CD3-positivity, respectively. For this, leukocytes were stained with either Pacific Blue-conjugated anti-CD19 or anti-CD3 (clones HIB19 and OKT3, BioLegend) together with staining for free GPI and GPI-APs.

For DNA and RNA analyses, granulocytes with PNH phenotype and normal granulocytes were separated by a cell sorter (FACSAria, BD). For this, the total blood leukocytes were stained by FLAER and subjected to cell sorting. Granulocytes were identified by their side and forward scatters and were separated into FLAER-negative and -positive fractions.

Determination of break points causing the 18 Mb deletion in patient J1
Genomic DNA of peripheral blood granulocytes from patient J1 containing 29% GPI-AP-deficient cells was used as a template for PCR to amplify a fragment including break points. All combinations of forward primers 1 to 3 and reverse primers 4 to 6 were used (positions and sequences of PCR primers in Figure S5**A**, top and Table S1). A fragment amplified with primers 1 and 5 (red arrowheads) was Sanger sequenced using primers 7 to 11 (positions and sequences in Figure S5**A**, top and Table S1).

Quantitative PCR (qPCR) analysis of chromosome 20q bearing the break points to determine the clone size of GPI-AP-deficient cells in patient J1
Two samples of J1's genomic DNA, one (sample #1) prepared from the whole blood leukocytes taken four months before the onset of recurrent hemolysis and the other (sample #2) prepared from granulocytes (29% GPI-AP-deficient) taken one month after the commencement of eculizumab therapy, were analyzed by qPCR. Primers to amplify a region including the break were designed based on the determined break points (Figure S5**A**). A region in exon 3 of PIGL was amplified as a reference. Primer sequences are shown in Table S1. SYBR Green Master Mix and StepOnePlus system (Thermo Fisher Scientific) were used. Ratios of (Break)/(PIGL) were determined for #1 and #2 samples with the $2(-\Delta\Delta Ct)$ method for comparative analysis, and a relative level of the break in #1 sample was determined setting a ratio of #2 sample as 1 (Results are shown in Figure 3**G**). Percent GPI-AP-deficient cells in the whole blood leukocytes at four months before the onset of recurrent hemolysis was determined by multiplying 29% by a relative level of the break in #1.

Generation and characterization of PIGTKO, PIGAKO and PIGT-SLC35A2 double KO THP-1 cells.
Gene disruption in THP-1 cells was made with CRISPR/Cas9 system (guide RNA sequences shown in Table S1). PIGTKO and PIGAKO cell clones were established based on their phenotypes (loss of FLAER- and CD55-positive staining) and mutations as assessed by Sanger sequencing. Specificities of KO were confirmed by

restoration of the wild-type phenotypes after transfection of corresponding cDNAs. PIGT-SLC35A2 double KO (PIGT-SLC35A2KO) cells were established by KO SLC35A2 in PIGTKO cells and sorting T5 mAb staining positive cells.

Quantitative RT-PCR (qRT-PCR) for IL1β and NLRP3
Levels of IL1β and NLRP3 mRNAs were analyzed by qRT-PCR using SYBR Green (Applied Biosystems) and appropriate primers (Table S1). Data were normalized to β–actin according to the 2(−ΔΔCt) method for comparative analysis. IL1β and NLRP3 mRNA levels of PMA-treated WT cells were set to 1. Result was expressed as the mean ± SD of duplicate determinations of a representative experiment.

Supplemental Results
Characterization of the patients' blood samples and bone marrow
Blood cell counts and neutrophil percentage in leukocytes of patients G1 and G3 were shown as a function of time in days in Figure S1**A**. LDH levels of patient G1 were also shown. Total leukocyte counts and platelet counts were within normal ranges in patients G1 and G3 (Figure S1**A**) and J1 (1), except at around severe hemolysis. The bone marrow specimen of patient G3, collected 6 months after the first meningitis episode and 4 years before the diagnosis of PNH showed an increased hematopoiesis. There were no signs of malignancy or aplasia. Taken together with reports that there were no signs of aplasia in the bone marrow of J1 (1) and G1 (2), bone marrow failure does not seem to be a feature of patients with PIGT-PNH.

Determination of break points causing the 18 Mb deletion in patient J1
The 18 Mb deletion was previously determined by a SNP array analysis of GPI-AP-deficient and GPI-AP-positive granulocytes from J1 (1). The SNP array analysis showed that SNPs at positions 31,905,813 and 49,909373 were present in the deletion-containing chromosome 20 of GPI-AP-deficient cells whereas all SNPs between those at 31,925,918 and 49,759,935 were absent (Figure S5**A**, top : positions according to GRCh37/hg19, NCBI/UCSC). Therefore, the centromeric and the telomeric break points must exit between positions 31,905,813 and 31,925,918, and positions 49,759,935 and 49,909373, respectively. To amplify a DNA fragment including the break points, we designed three PCR primers each in the centromeric (primers 1 to 3) and the telomeric (primers 4 to 6) regions (Figure S5**A**, top). Using genomic DNA from J1 granulocytes containing 29% GPI-AP-deficient cells as a template (sample #2 in Figure S5**B**, right part), PCR with primers 1 and 5 (primer set 1-5) generated a 6-kbp product (marked *) whereas PCRs with all other primer sets gave negative results or non-specific products. To determine nucleotide sequence of the 6-kbp PCR product, we generated five sequence primers (7 to 11 in Figure S5**A**, top). Sequencing with primer 8 (red) was successful. Two break points at positions 31,909,463 and 49,798,761, and an insertion of five nucleotides (5'-ACATT) between the break points were identified (Figure S5**A**, bottom).

A clone size of GPI-AP-negative leukocytes in patient J1 at four months before the onset of recurrent hemolysis
We also used J1's genomic DNA prepared from the whole blood leukocytes taken four months before the onset of recurrent hemolysis (sample #1 in Figure S5**B**, left part) as a template in PCR. Similar to sample #2, primer set 1-5 generated a 6-kbp product (marked *) whereas all other primer sets gave negative results or non-specific

products (Figure S5**B**, left part). The 6-kbp product amplified from sample #1 was confirmed to be the same break-containing region by Sanger sequencing. The amount of the 6-kbp product from sample #1 was much smaller than that from sample #2 (29% GPI-AP-deficient cells). These results indicate that J1 had a small GPI-AP-clone four months before the onset of PNH.

To determine the clone size at four months before the onset of recurrent hemolysis, we analyzed samples #1 and #2 by qPCR. The level of the break-containing DNA in sample #1 was approximately 10% of sample #2 (Figure 3**G**), indicating approximately 3% of total leukocytes were GPI-AP-deficient.

Characterization of PIGTKO, PIGAKO and PIGT-SLC35A2 KO THP-1 cells
The surface expressions of GPI-APs were lost from both PIGTKO and PIGAKO cells and were restored by transfection of *PIGT* and *PIGA* cDNAs, respectively (Figure S6**A**). PIGTKO, PIGAKO and wild-type (WT) THP-1 cells were differentiated into macrophages by phorbol 12-myristate 13-acetate (PMA) to induce competence in inflammasome activation (3). They were then tested by priming with Pam_3CSK_4 followed by 4h-treatment with ATP. IL1β was released at similar levels from WT, PIGTKO and PIGAKO cells (167.9±61.5, 144.3±19.7, 200.3±48.8 pg/ml), indicating that they have comparable abilities to respond to inflammasome activators (Figure S6**B**). PIGT-SLC35A2KO cells were strongly stained by T5 mAb whereas PIGTKO cells were only very weakly stained by T5 mAb (Figure S6**C**). This result indicated that most free GPIs in PIGTKO cells were not detected by T5 mAb because of capping by galactose (schematic shown in Figure 3**A**).

IL1β and NLRP3 levels in PIGTKO, PIGAKO and WT THP-1 cells before and after incubation with complement
Transcriptional induction of IL1β and NLRP3 were at similar levels in PIGTKO, PIGAKO and wild-type (WT) THP-1 cells and the PIGTKO cells rescued by PIGT cDNA. IL1β was induced by PMA alone, while NLRP3 induction was further enhanced by the acidified serum (Figure S7**A**).
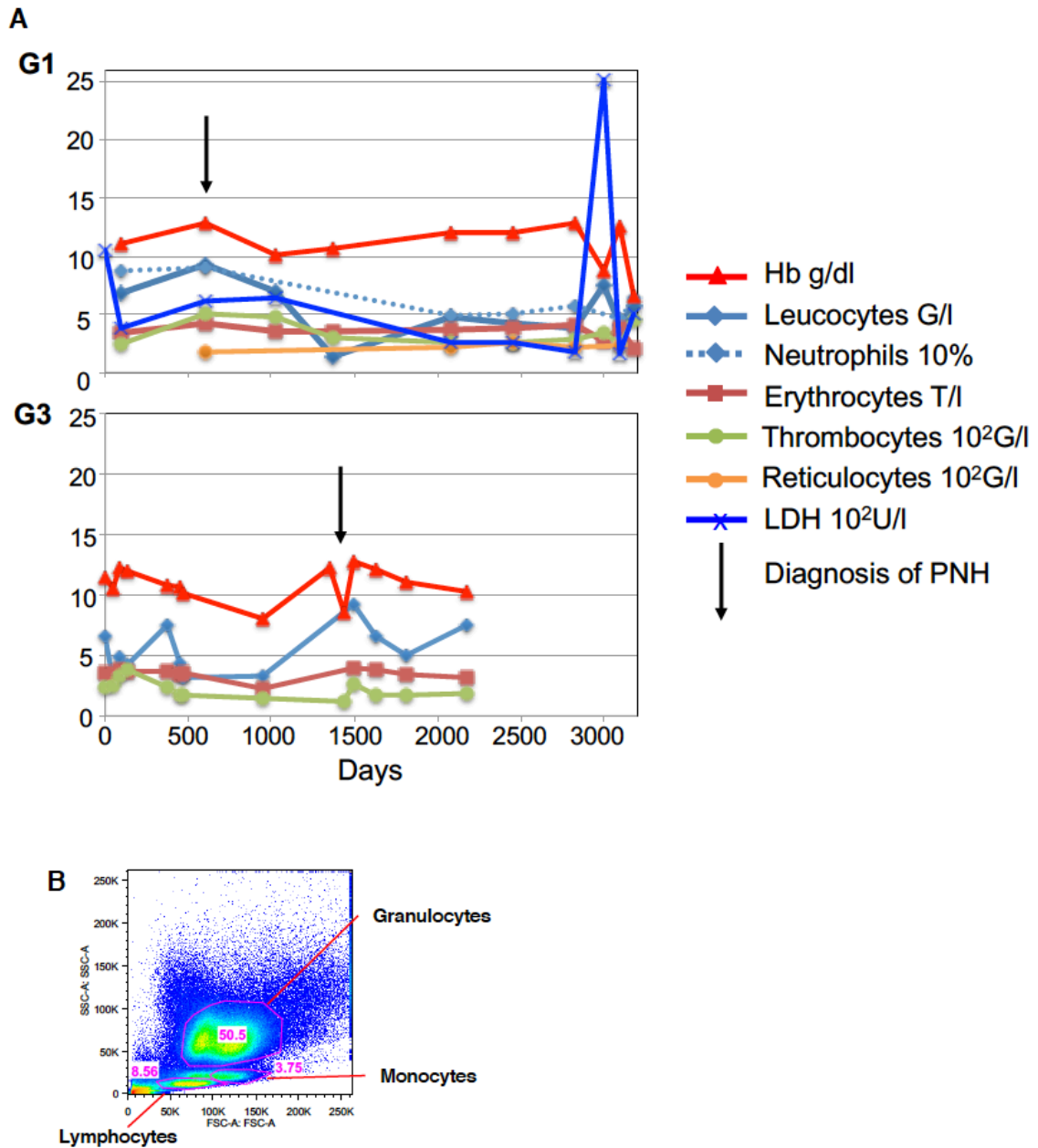
Fig. S1. Blood cell counts in patients G1 and G3 and gating of peripheral blood cells. A. Time course of blood cell counts. A very high peak of LDH found in patient G1 on around day 3000 was caused by severe hemolytic crisis occurred after a transient extension of the eculizumab therapy interval (2). G/l, billion cells per liter; 10^2G/l, hundred billion cells per liter; T/l, trillion cells per liter. **B.** Gating of granulocyte, monocyte and lymphocyte populations based on forward (FSC) and side (SSC) scatters.
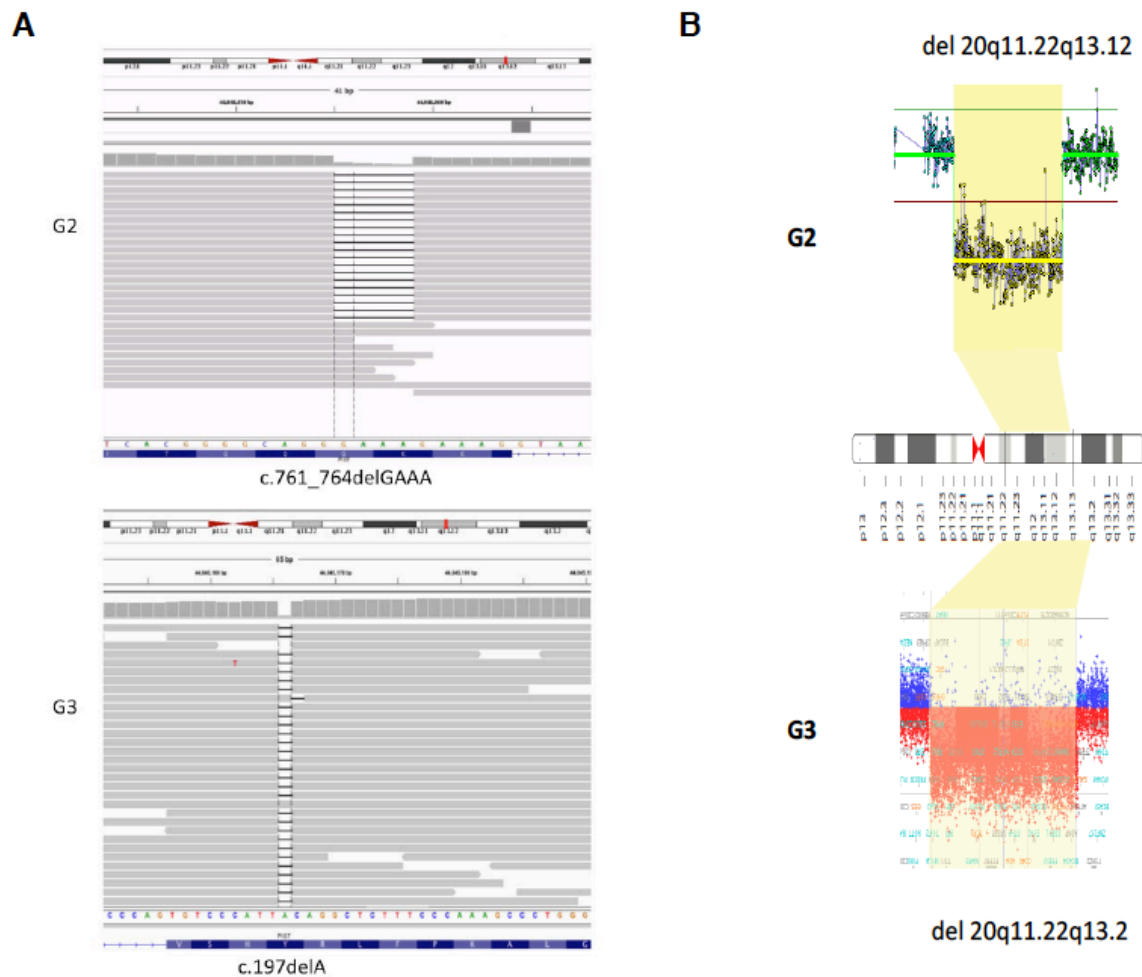
Fig. S2. Rare pathogenic variants and somatic mutations of *PIGT* in PIGT-PNH G2 and G3 revealed by Gene Panel analysis and array comparative genomic hybridization. A. The inherited variants in G2 and G3 are a four-base pair deletion (NM_015937: c.761_764delGAAA) and a one-base pair deletion (NM_015937: c.197delA) in *PIGT*. **B.** The somatic deletion in G2 spans over 12 Mb on chr 20q and involves *PIGT* and *PIGU,* arr[hg19] 20q11.22q13.12(32,837,289-44,973,145)x1. The somatic event in G3 is a 15 Mb deletion involving *PIGT*, arr[hg19] 20q11.22q13.2(34,975,105-50,140,767) x1.
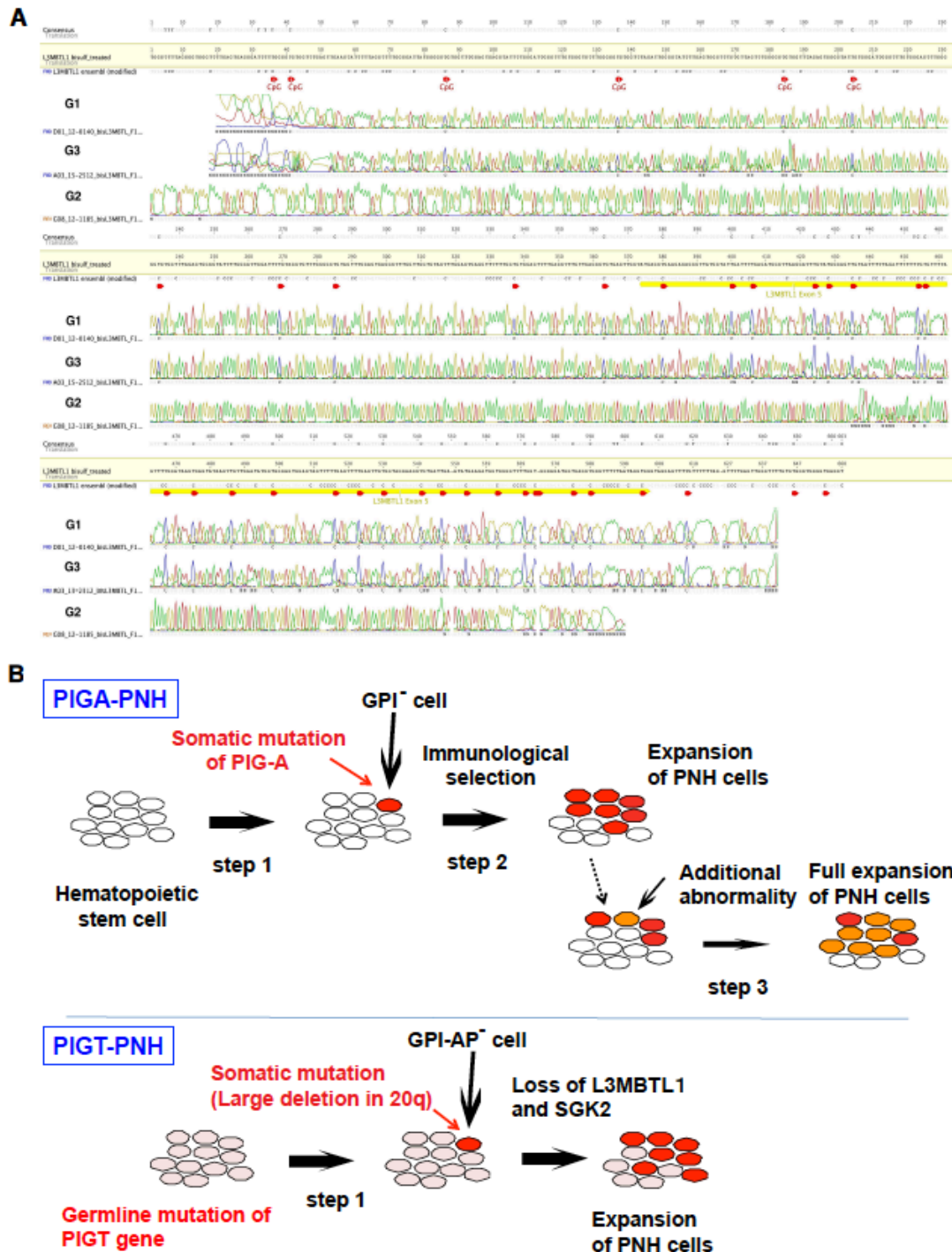
Figure S3. Methylation status of *L3MBTL1* and a model for clonal expansion in PIGT-PNH. A. Bisulfite sequencing of the informative region in *L3MBTL1* in G1, G2 and G3. **B**. Models of clonal expansion of GPI-defective cells in PNH (top) and PIGT-PNH (bottom). In PNH, somatic mutation of *PIGA* gene in a hematopoietic stem cell generates GPI-defective clone (step 1). Under bone marrow failure conditions, normal stem cells are damaged by autoimmune mechanisms whereas GPI-defective clone survives, causing clonal expansion (step 2). In some cases of PNH, GPI-defective subclone that acquired benign-tumor-like growth phenotype expands greatly (step 3). In PIGT-PNH, patients had a germ line loss-of-function mutation in the maternal allele of *PIGT*. A deletion spanning the entire *PIGT* and myeloid

common deletion region occurs in the paternal allele in a hematopoietic stem cell, generating GPI-AP-defective clone (step 1). Because of losses of maternally imprinted *L3MBL1* and *SGK2* genes, the GPI-AP-defective clone may obtain a competence to expand and may initially contribute to non-erythrocytic myeloid cells causing recurrent autoinflammation. Years later, *PIGT*-defective clone may begin to generate sufficient numbers of GPI-AP-defective erythrocytes to cause PNH phenotype.
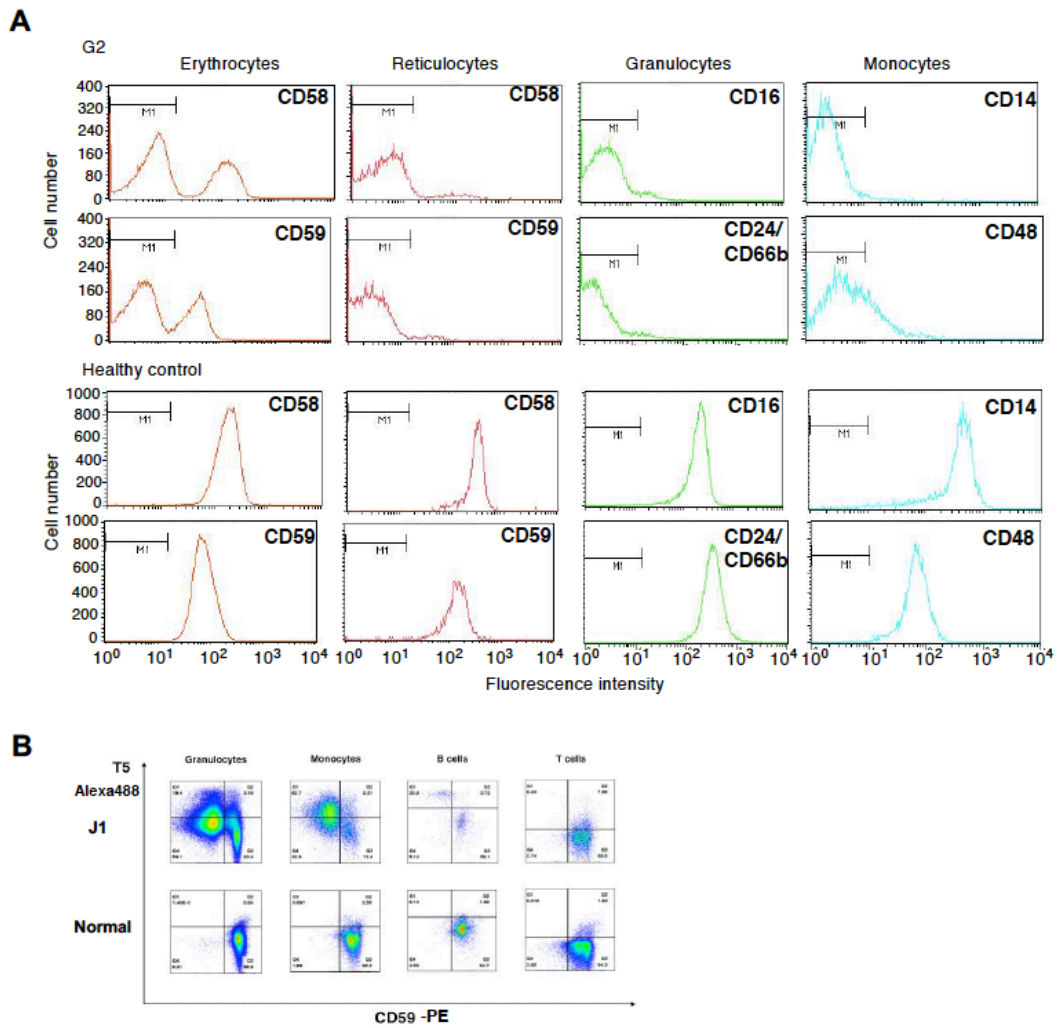
Figure S4. Flow cytometry of blood cells from patients with PIGT-PNH. A.
Peripheral blood cells from G2 with PIGT-PNH (top two lows) and a healthy control
(bottom two lows) were stained for GPI-APs. **B**. Granulocytes, monocytes, B- and T-
lymphocytes from J1 with PIGT-PNH and a normal individual, stained by T5 mAb
and anti-CD59 mAb.
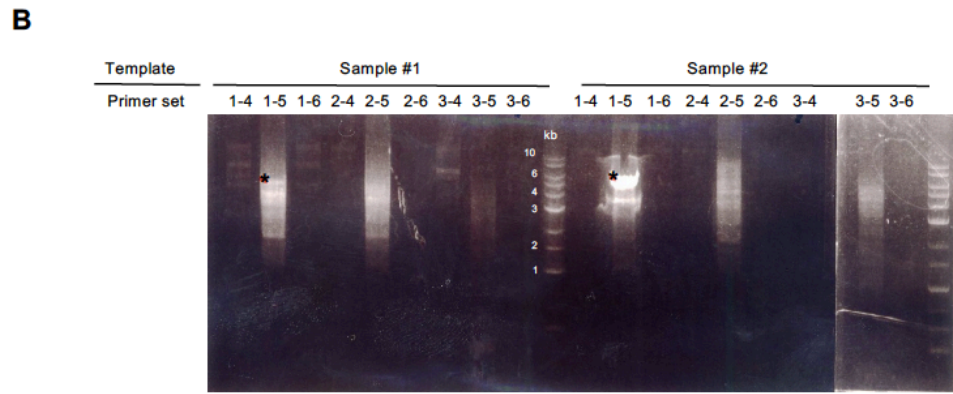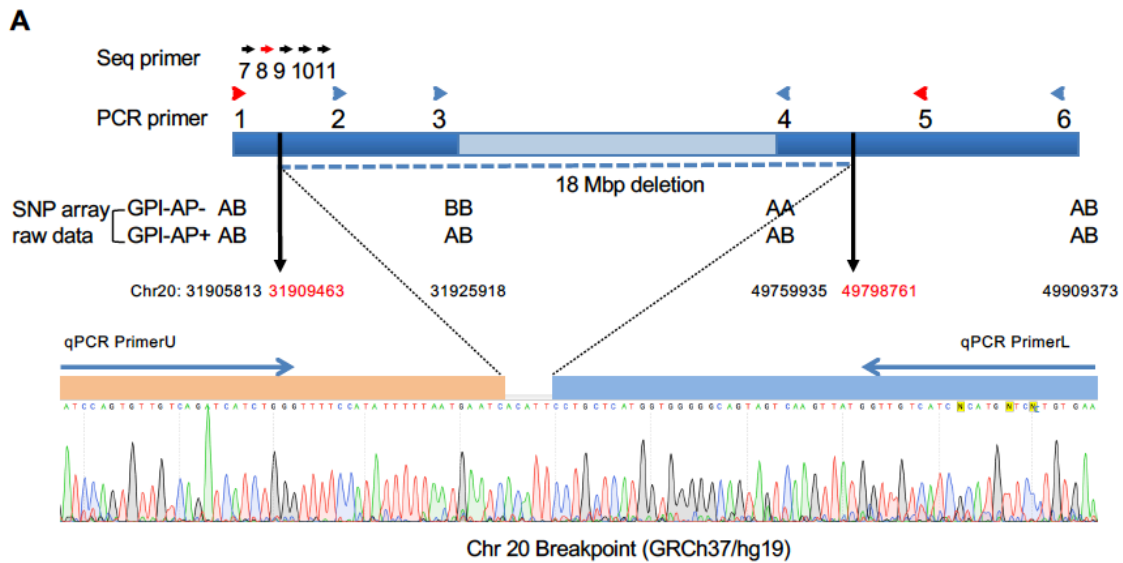
Figure S5. Determination of the break points causing the 18 Mb deletion in J1. A (Top) Schematic of a region in patient J1's chromosome 20q bearing the 18 Mb deletion (centromere on the left). Four informative SNPs (AB, heterozygous; AA and BB, homozygous) are shown in their position numbers below the schematic: SNPs heterozygous in both GPI-AP-positive and GPI-AP-deficient cells (at 31,905,813 and 49,909,373) were present in GPI-AP-deficient cells whereas those homozygous in GPI-AP-deficient cells and heterozygous in GPI-AP-positive cells (at 31,925,918 and 49,759,935) were within the deleted region in GPI-AP-deficient cells. PCR primers 1 to 6 used to amplify a region including break points are shown immediately above the schematic. Sequence primers 7 to 11 used to determine nucleotide sequence of the PCR product with primers 1 and 5 (red arrowheads) (see **B** for PCR products) are shown on top: sequencing with primer 8 (red) was successful. (Bottom) Sanger sequence result with primer 8. Two break points at positions 31,909,463 and 49,798,761, and an insertion of five nucleotides (5'-ACATT) between the break points were identified. Locations of primers for qPCR (Primers U and L) to determine the clone size of GPI-AP- cells are shown above the sequence. **B**. PCR products from template samples #1 and #2 with all combinations of primers. Sample #1, genomic DNA from the whole blood leukocytes taken four months before the onset of recurrent hemolysis; sample #2, genomic DNA from granulocytes (29% GPI-AP-deficient) taken one month after the commencement of eculizumab therapy. PCR with primer set 1-5 generated a 6 kbp product strongly from sample #2 and weakly from sample #1. All other primer sets gave negative results or non-specific products.

10
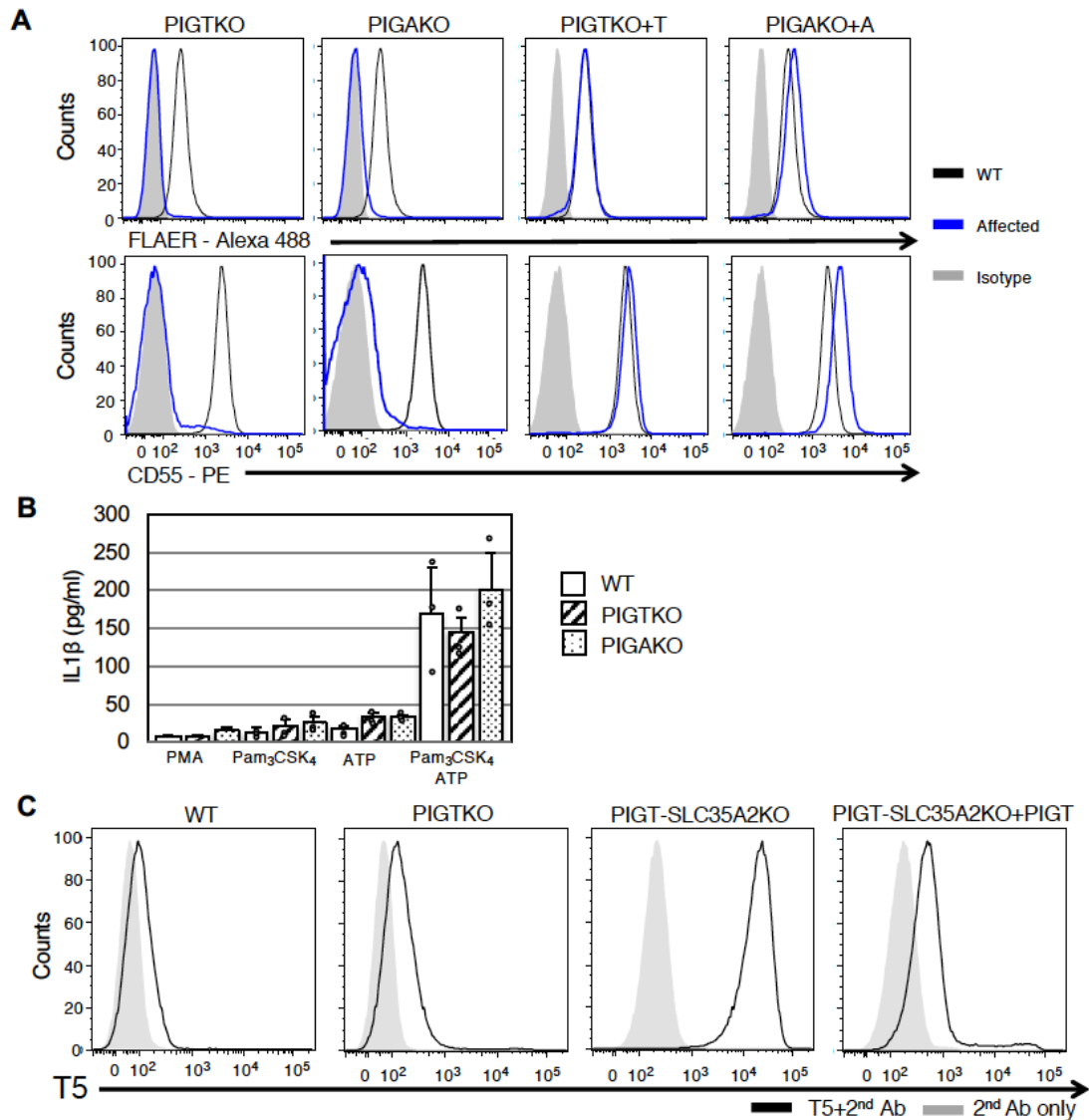
Figure S6. Characterization of PIGT and PIGA knockout THP-1 cells. A. Surface expression of GPI-APs on PIGT knockout (KO), PIGAKO and PIGT- / PIGA-rescued (PIGTKO+T, PIGAKO+A) THP-1 cells. Test cells (blue lines) and wild-type cells (solid lines) were stained with FLAER (top panels) and PE-labeled anti-CD55 antibody (bottom panels). Negative staining controls (shaded) for FLAER and anti-CD55 were buffer only and isotype matched monoclonal antibody, respectively. The expressions of GPI-APs on PIGTKO and PIGAKO cells were lost and normalized by rescue transfections of relevant cDNAs. **B**. Secretion of IL1β from THP-1 cells. WT, PIGTKO and PIGAKO THP-1 cells were differentiated into macrophages by PMA (100 ng/ml). The differentiated cells were primed with Pam_3CSK_4 (200 ng/ml) for 4 hr, after which medium was removed and pulsed for 4 hr with ATP (5mM). IL1β released into medium was measured by ELISA. Data are expressed as mean + SD of three independent experiments. **C**. Expression of free GPI on WT, PIGTKO, PIGT-SLC35A2 KO, PIGT-rescued PIGT-SLC35A2 KO THP-1 cells. T5 mAb did not positively stain WT and PIGTKO THP-1 cells whereas it stained PIGTKO-SLC35A2KO THP-1 cells strongly. SLC35A2KO cells derived from PIGTKO cells are defective in galactosylation because of defective UDP-Gal transporter encoded by *SLC35A2*, indicating that PIGTKO THP-1 cells express free GPI whose GalNAc side-chain is fully galactosylated.

11
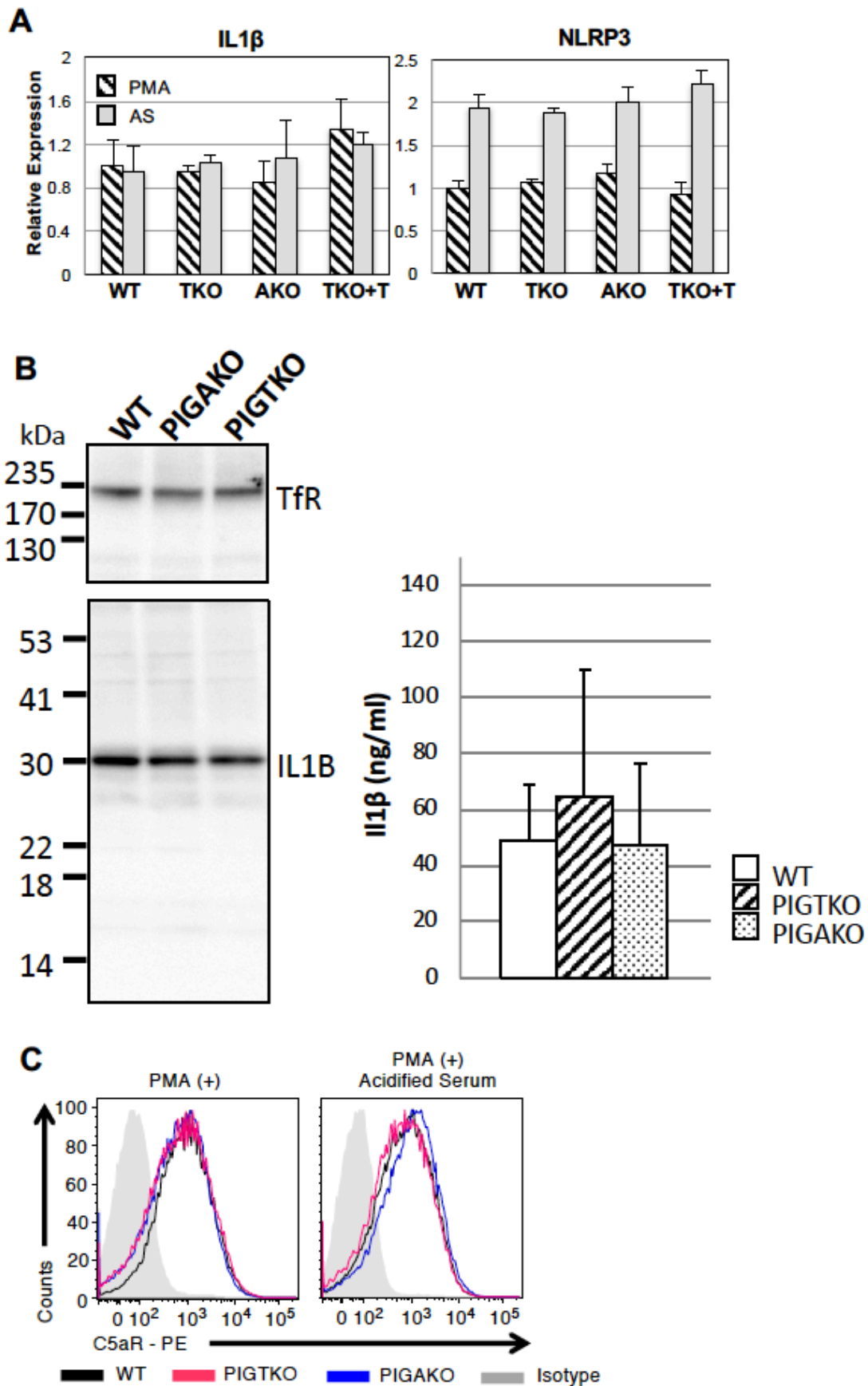
Figure S7. Responses of THP-1 cells to complement. A. Levels of IL1β and NLRP3 transcripts in WT, PIGTKO, PIGAKO and PIGT-rescued PIGTKO THP-1 cells. Cells were differentiated to macrophages by PMA and RNA prepared before

(hatched bars) and after (grey bars) 5-hr incubation in 50% acidified serum (AS). IL1β (left) and NLRP3 (right) transcripts were measured by qRT-PCR. Data are expressed as mean + SD of triplicate samples from one of three independent experiments. **B**. Levels of IL1β protein in WT, PIGTKO and PIGAKO THP-1 cells. After differentiation by PMA, detergent extracts were prepared and IL1β determined by western blotting (left) and ELISA (right). TfR, transferrin receptor used as a loading control. Levels of IL1β determined by ELISA were expressed as mean + SD of three independent experiments. **C**. Levels of C5aR on THP-1-derived macrophages before and after incubation in acidified serum. WT (black lines), PIGTKO (red lines) and PIGAKO (blue lines) cells before (left) and after 5-hr incubation in 50% acidified serum (right) were stained by anti-CD88 mAb. Shaded, WT cells stained by isotype control antibody. Mean + SD of three independent experiments.
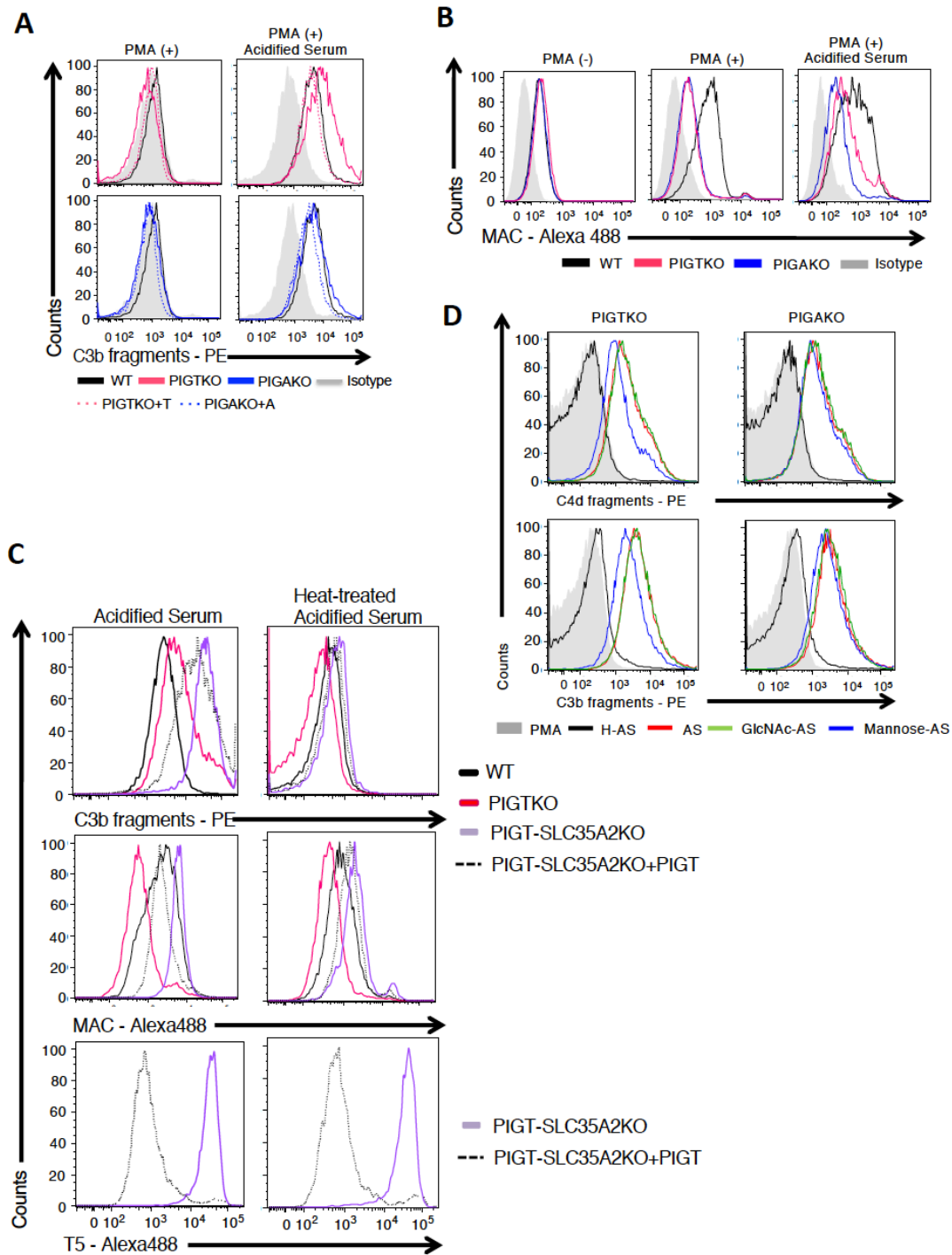
Figure S8. A. Detection of C3b fragments by flow cytometry. THP-1 cells were differentiated into macrophages by PMA (left) and incubated with 50% acidified serum for 5 hr after differentiation (right). WT (black lines), PIGTKO (solid red lines), PIGT-rescued PIGTKO (dotted red lines), PIGAKO (solid blue lines) and PIGA-rescued PIGAKO (dotted blue lines). One representative experiment of three independent experiments. **B**. Detection of MAC by flow cytometry. WT (black lines), PIGTKO (red lines), PIGAKO (blue lines) THP-1 cells were left undifferentiated (left), differentiated into macrophages by PMA (center) and incubated with 50% acidified serum for 5 hr after differentiation (right). One representative experiment of three independent experiments. **C**. Detection of C3b fragments (top), MAC (middle)

and free GPI (bottom) on PIGT-SLC35A2 KO THP-1 cells and PIGT-rescued PIGT-SLC35A2 KO THP-1 cells after PMA-treatment and incubation with acidified serum (left) or heated acidified serum (right). Black lines, WT; red lines, PIGTKO; purple lines, PIGT-SLC35A2 KO; dotted lines, PIGT-rescued PIGT-SLC35A2 KO. **D**. Detection of C4d (top) and C3b fragments (bottom) on PIGTKO (left) and PIGAKO (right) THP-1 macrophages after AS treatment. Shaded, non-treated cells; black lines, heat-inactivated AS (H-AS); red lines, AS; green lines, AS with 100mM N-acetylglucosamine (GlcNAc-AS); blue lines, AS with 100 mM mannose (Mannose-AS).

Table S1. Table S1. Sequences of primers and guide RNA used in this study.

qPCR primers

cDNA	Sequence (5'-3')
ABL-F	GCGTGAGAGTGAGAGCAG
ABL-R	TCTCGGAGGAGACGTAG
SGK2E9F	CTGAAGTGCTTCGGAAAGAG
SGK2E10R2	CGGCTGGTGCAGAATGTTC
L3MBTLE10F2	TGTACTTCATCCTCACCGTG
L3MBTLE11R1	AGTTGGCATTGACCCAGAAG
IFT52E6F2	TGCCTGGGATCATTGATGAG
IFT52E7R1	ACAGAACCTGTAGACAGAAC
MYBL2 4F1	AATGCCAGTACAGGTGGCTG
MYBL2 5R1	TTCAGGTGCTTGGCAATCAG
β actin–F	AGAGCTACGAGCTGCCTGAC
β actin–R	AGCACTGTGTTGGCGTACAG
IL-1β-F	TTACAGTGGCAATGAGGATGAC
IL-1β-R	GTCGGAGATTCGTAGCTGGAT
NLRP3-F	CGTGAGTCCCATTAAGATGGAGT
NLRP3-R	CCCGACAGTGGATATAGAACAGA
chr20 breakU	ATCCAGTGTTGTCAGATCATCTGGG
chr20 breakL	TTCACAGGAACATGCGATGACAACC
hPIGLex3U	GGATTTCCCAGATGACCCAG
hPIGLex3L	CAGATTGATGCCATTCACTTCT

Primers for the break point determination

1 (chr20-1-31905941U)	TGGACCACCTGCCCTTTGTAGG
2 (chr20-2-31915901U)	AGGCAGGGTAGAGATGCTGAAATC
3 (chr20-3-31925781U)	CCCTGAGTATTGACATCTGTGAGCA
4 (chr20-1-49769935L)	GCTTACTGAATGATCACAAAGCAAGCT
5 (chr20-2-49800157L)	GTTAGGACCACATTTGCCCACAGG
6 (chr20-3-49900000L)	TTAGGGGTGGTCCCATGACTTACTTC
7 (chr20-4U)	TTCCAGCTGACTGGGAGGCT
8 (chr20-5U)	GATCTGGGCTCACCACAACCT
9 (chr20-6U)	GACTCGCCCTCCTGACTGCA
10 (chr20-7U)	CCACAACAGCTGACAAGTATATGGC
11 (chr20-8U)	GAACACAAATTCTTCTCCTGTTCTGACC

Guide RNA sequence

Target gene	Sequence (5'-3')
hPIGT Cas 212U	**CACC** gaatgtggcggctacgtccccgg
hPIGT Cas 212L	**AAAC** ccggggacgtagccgccacattc
hPIGA Cas 190U	**CACC** ccagggctaacccgagagagtgt

hPIGA Cas 190L	**AAAC** acactctctcgggttagccctgg
hSLC35A2 FW-4	**CACC** ggtggttccaccgcggcgcc
hSLC35A2 RV-4	**AAAC** ggcgccgcggtggaaccacc

Table S2. PIGT mutations in Inherited GPI Deficiency (IGD)

Family	Origin	M[A)] allele	P[A)] allele	Reference
1	Aramaic	c.547A>C[B)] (p.T183P)	c.547A>C (p.T183P)	Kvarnung (4)
2	Japanese	c.250G>T[C)] (p.E84*)	c.1342C>T (p.R448W)	Nakashima (5)
3	Caucasian (M)/African American	c.918dupC (p.V307Rfs*13)	c.1342C>T (p.R448W)	Lam (6)
4	Somalian	c.1079G>T (p.G360V)	c.1079G>T (p.G360V)	Skauli (7)
5	Caucasian	c.1582G>A (p.V528M)	c.1730dupC (p.L578fs*35)	Pagnamenta (8)
6	Afghan	c.709G>C (p.E237Q)	c.709G>C (p.E237Q)	Pagnamenta (8)
7	Japanese	c.250G>T[3)] (p.E84*)	c.1096G>T (p.G366W)	Kohashi (9)
8	Chinese	c.550G>A (p.E184K)	c.550G>A (p.E184K)	Yang (10)
9	NI[D)]	c.1484+2T>A	c.1472T>A (p.L491H)	Bayat (11)
10	Polish	c.1582G>A (p.V528M)	c.494-2A	Bayat (11)
11	Polish	c.1582G>A (p.V528M)	c.1582G>A (p.V528M)	Bayat (11)
12	NI	c.1079G>T (p.G360V)	c.1079G>T (p.G360V)	Bayat (11)
13	NI	c.1079G>T (p.G360V)	c.1079G>T (p.G360V)	Bayat (11)
14	Polish	c.1730dupC (p.L578fs*35)	c.1582G>A (p.V528M)	Bayat (11)
15	Pakistani	c.550G>A (p.E184K)	c.550G>A (p.E184K)	Bayat (11)
16	Bangladeshi	c.709G>C (p.E237Q)	c.709G>C (p.E237Q)	Bayat (11)

[A)] M, maternal; P, paternal

[B)] Based on NM_015937

[C)] The same mutation was found in patient J1 with autoinflammation-paroxysmal nocturnal hemoglobinuria (PIGT-PNH) (Table 1).

[D)] Not Identified

References

1. Kawamoto M, Murakami Y, Kinoshita T, & Kohara N (2018) Recurrent aseptic meningitis with PIGT mutations: a novel pathogenesis of recurrent meningitis successfully treated by eculizumab. *BMJ Case Rep* 2018(doi: 10.1136/bcr-2018-225910).

2. Krawitz PM*, et al.* (2013) A case of paroxysmal nocturnal hemoglobinuria caused by a germline mutation and a somatic mutation in PIGT. *Blood* 122(7):1312-1315.

3. Zhou R, Yazdi AS, Menu P, & Tschopp J (2011) A role for mitochondria in NLRP3 inflammasome activation. *Nature* 469(7329):221-225.

4. Kvarnung M*, et al.* (2013) A novel intellectual disability syndrome caused by GPI anchor deficiency due to homozygous mutations in PIGT. *J Med Genet* 50(8):521-528.

5. Nakashima M*, et al.* (2014) Novel compound heterozygous PIGT mutations caused multiple congenital anomalies-hypotonia-seizures syndrome 3. *Neurogenetics* 15(3):193-200.

6. Lam C*, et al.* (2015) Expanding the clinical and molecular characteristics of PIGT-CDG, a disorder of glycosylphosphatidylinositol anchors. *Mol Genet Metab* 115(2-3):128-140.

7. Skauli N*, et al.* (2016) Novel PIGT variant in two brothers: Expansion of the multiple congenital anomalies-hypotonia seizures syndrome 3 phenotype. *Genes (Basel)* 7(12):pii: E108.

8. Pagnamenta AT*, et al.* (2017) Analysis of exome data for 4293 trios suggests GPI-anchor biogenesis defects are a rare cause of developmental disorders. *Eur J Hum Genet* 25(6):669-679.

9. Kohashi K*, et al.* (2018) Epileptic apnea in a patient with inherited glycosylphosphatidylinositol anchor deficiency and PIGT mutations. *Brain Dev* 40(1):53-57.

10. Yang L*, et al.* (2018) Homozygous PIGT Mutation Lead to Multiple Congenital Anomalies-Hypotonia Seizures Syndrome 3. *Front Genet* 9:153.

11. Bayat A*, et al.* (2019) PIGT-CDG, a disorder of the glycosylphosphatidylinositol anchor: description of 13 novel patients and expansion of the clinical characteristics. *Genet Med* 2019, doi 10.1038/s41436-019-0512-3.